2011 IEEE International Conference on Robotics and Automation
Shanghai International Conference Center
May 9-13, 2011, Shanghai, China

Meso-scale Compliant Gripper Inspired by Caterpillar's Proleg

Gwang-Pil Jung, Je-Sung Koh, and Kyu-Jin Cho

Abstract—**We propose a biomimetic gripper, inspired by a caterpillar's proleg, that can reliably grip dusty and rough terrain. A caterpillar's proleg makes this possible by using a retractor muscle that opens and closes the proleg, and a planta that gives compliance to the proleg. We implement these components with shape memory alloy (SMA) coil actuators and flexure joints. The gripper is fabricated using composite links and flexure joints. This method replaces metal-based joints and links with flexure joints and composite-based rigid links. The composite-based design provides a simple, light weight, and compact structure that enables the gripper to be applied to small-scale robots. Modeling and experiments are used to analyze the gripping force. The results show how the gripping force changes depending on the length of the flexure joint. A prototype was built to demonstrate reliable gripping on a rough-surfaced block using an adaptive mechanism.**

I. Introduction

MANY bio-inspired robots use gripping or attaching devices to climb and maneuver on rough, dusty, and inclined surfaces. These robots employ various gripping mechanisms such as adhesive pads [1], [2], suction devices [3], [4], magnets [5], and spines [6]. However, except for the spine-based robots, these methods are only suitable for attaching to smooth, clean, and even surfaces. To grip a wide range of surfaces, we focused on a spine-based gripper that is useful for gripping the dusty, rough, and uneven surfaces that typically exist in nature.

Many insects and animals employ spines for reliable gripping. At a small scale, beetles have a tarsal claw system to generate friction force [11], and caterpillars use crochets in their prolegs [10]. At a large scale, members of cat families such as tigers, lions, leopards, and cheetahs have solid claws for gripping.

As a biological gripper model, we chose a caterpillar's proleg. A caterpillar's proleg has a simple mechanism and is small in size. A retractor muscle attached through the center of the proleg opens and closes the proleg. Planta, located below the points where the crochets or the spines are attached, provides compliance to the crochets. This compliance enables adaptive gripping. These two simple but effective features are implemented in our gripper design to enable adaptive gripping on a small scale.

The proposed bio-inspired gripper was fabricated using smart composite microstructure (SCM) process [8]. Smart composite microstructure makes it possible to replace metal-based pin joints and links with flexure joints and composite-based links. Also, by installing a shape memory alloy (SMA) coil actuator inside the gripper, the structure becomes more compact. Using the SCM process and the SMA coil actuator, the gripper can be applied to small-scale robots such as the Omegabot [7], as shown in Fig. 1. The weight of the gripper is only 0.45 g.

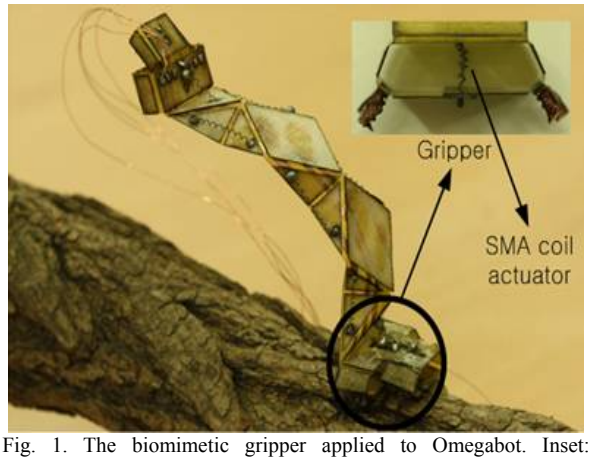

Fig. 1. The biomimetic gripper applied to Omegabot. Inset: magnification of the gripper

Modeling of the gripping structure was achieved using a pseudo-rigid body model (PRBM) [12]. The PRBM provides a simple method of analyzing structures that undergo large nonlinear deflections. The PRBM replaces a flexure beam with a torsional spring and a pseudo-rigid-body link. Using the PRBM, a kinematic model and a force-deflection model of the gripping structure were developed.

For adaptive and reliable gripping, we investigated how the compliance of the gripper changes depending on various lengths of the middle flexure joint. This experiment provides useful information on how to adjust compliance by changing the length of the flexure joint. A prototype was built to demonstrate the reliability of the gripping mechanism.

II. Biological Model And Concept Design

Caterpillars employ crochets in the apical area (near the tip) of the proleg. Fig. 2 shows the transverse section through part of an abdominal segment of a caterpillar showing a proleg. The main components used in generating the gripping motion are the retractor muscles inside the proleg's outer wall and the planta in the apical area.

The authors are with the School of Mechanical and Aerospace Engineering, Seoul National University (e-mail: ceaser97, kjs15, kjcho@snu.ac.kr).

978-1-61284-385-8/11/$26.00 ©2011 IEEE

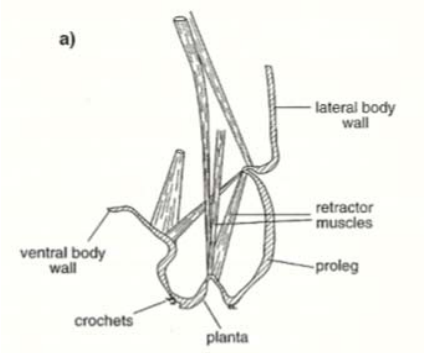

Fig. 2. Transverse section through part of an abdominal segment of a caterpillar showing a proleg [9].

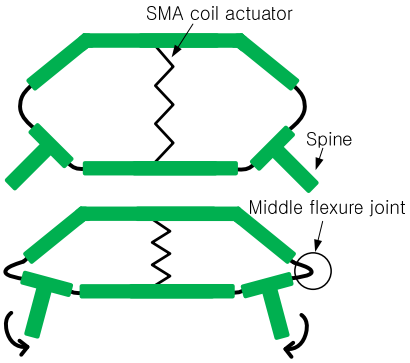

Fig. 3. Conceptual design of the bio-inspired gripper.

The planta features rows of crochets that have the ability to grip. Also, the planta is less rigid compared to the side of the proleg. Due to these attributes, the proleg can achieve reliable and compliant gripping on a rough surface. The retractor muscles are located at the center of the planta so that they can disengage the crochets inwardly when they contract.

Inspired by the caterpillar's proleg, we propose a biomimetic gripper that is made of rigid links and flexure joints as shown in Fig. 3. The SMA coil actuator works as a retractor muscle, and the middle flexure joint serves as the planta, thereby giving compliance to the caterpillar's proleg. Also, the spines are attached at the composite-based rigid links. When the SMA coil actuator contracts, the spines gather into the center of the gripping structure. With this motion, the bio-inspired gripper grips a surface like a real caterpillar.

III. Gripping Structure Analysis

Analyzing the proposed compliant gripping structure is challenging because of the large deflection of the flexure joints. To analyze the large deflection, a nonlinear analysis should be considered. A pseudo rigid body model (PRBM) [12] provides a simple and straightforward method of analyzing systems that undergo large and nonlinear deflections.

The PRBM replaces the flexure joint with flexural pivots, tensural pivots [16], [17], and a pseudo-rigid-body link. Also, the force-deflection relationship can be described using the

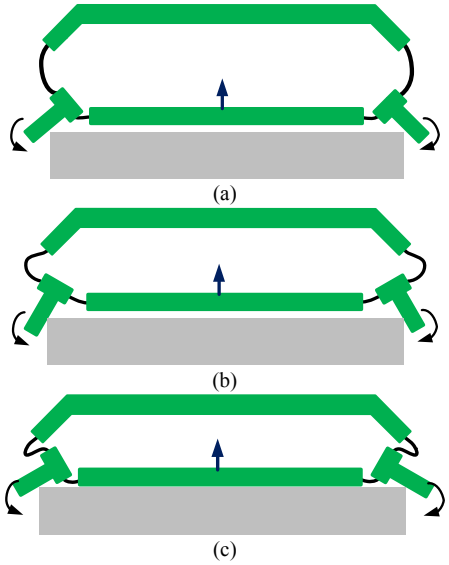

Fig. 4. The gripping process. (a) Before gripping. (b) Shortly after contact. (c) Buckling of flexure joint after fully gripping a block.

PRBM and the principle of virtual work.

A. Compliance of the Bio-inspired Gripper

Compliance is the critical factor for gripping devices because compliance makes it possible to grasp an object reliably and adaptively. In this bio-inspired gripper, buckling of the middle flexure joint has to do with compliance.

Fig. 4 shows how the gripper grasps an object using buckling and simple bending. In Fig. 4, (a) shows the gripper before gripping, and (b) shows gripping in the air. Fig. 4(c) shows buckling after gripping a block. In Fig. 4(c), buckling of the middle flexure joint adds an additional degree of freedom (DOF). This additional DOF provides more compliance to the gripper, which is important for adaptive gripping.

Fig. 5 is an enlarged image showing how the middle flexure joint changes during gripping. In Fig. 5, angle θ_3 holds its angle from shortly after the spine makes contact to shortly before buckling occurs. During this time, the gripping force increases

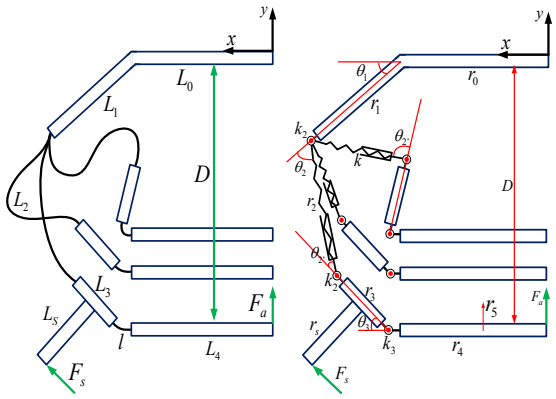

(a) (b)

Fig. 5. PRBM of a flexure joint in end-moment loading condition. (a) Flexure joint. (b) PRBM of flexure joint.

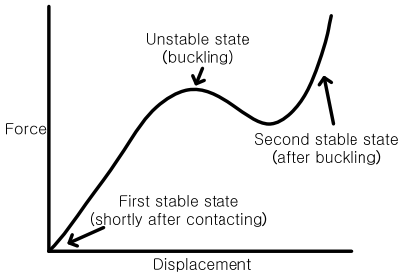

Fig. 6. Force-displacement relationship for bi-stable mechanism.

linearly. However, after buckling, the angle θ_3 varies and the gripping force does not increase further and even decreases, depending on the length of the middle flexure joint. After enough buckling, a tension is applied to the middle flexure joint because of the geometry of the gripping structure. Therefore, the gripping force again increases significantly.

The middle flexure joint of the gripper undergoes buckling as well as simple bending during grasping. Due to the buckling, the gripping force varies nonlinearly. This phenomenon can be modeled as a bi-stable mechanism. Fig. 6 shows the force-displacement relationship of the bi-stable mechanism. The initial state (shortly after contact) can be regarded as the first stable state, and the final state (after buckling) is treated as the second stable state. Buckling occurs in the unstable state in the middle of two stable states.

B. Pseudo Rigid Body Model of Gripping Structure

The middle flexure joint, L_2, can be replaced with a tensural pivot that includes two torsional springs and one linear spring, and is treated as a fixed-guided segment. l is replaced with a short flexural pivot since it is much shorter than other rigid links.

The location of the torsional spring, called the characteristic pivot, and the length of each rigid link are defined using a characteristic radius factor, γ. In the PRBM, it is important to determine the location of the flexural pivot and the length of each rigid link. These are defined using the characteristic radius factor γ, and the constant of the flexural pivot is determined by γ and the stiffness coefficient K_θ. Stiffness of the linear spring, k, can be determined experimentally and the other spring constants are given by

$$k_2 = 2\gamma K_\theta \frac{EI_2}{L_2} \tag{1}$$

$$k_3 = \frac{EI_l}{l} \tag{2}$$

The gripping force generated by the spine can be derived using the principle of virtual work. Generalized coordinates q are chosen as $q_1 = r_5$, $q_2 = \theta_3$ since r_5 and θ_3 are known input values.

As shown in Fig. 5, the SMA coil actuator generates actuation force , F_a, which is applied at the center of the lower rigid link. The gripping force applied to the spine, F_s, can be determined as an output of displacement caused by the actuation force. The following equations are derived depending on δq:

$$F_s r_s + k(r_2 - r_{20}) r_3 S_{2'} - k_2 \frac{r_3}{r_2} C_{2'}(\theta_2 - \theta_{2'}) + k_2\theta_2 - k_3\theta_3 = 0 \tag{3}$$

$$F_s S_3 + F_a + k(r_2 - r_{20}) S_{\pi-1-2} - k_2 \frac{1}{r_2} C_{\pi-1-2}(\theta_2 - \theta_{2'}) = 0 \tag{4}$$

The geometric relations can be derived as follows:

$$\theta_1 + \theta_2 + \theta_{2'} + \theta_3 = \pi \tag{5}$$

$$r_1 C_1 - r_2 C_{\pi-1-2} - r_3 C_3 = 0 \tag{6}$$

$$r_1 S_1 + r_2 S_{\pi-1-2} + r_3 S_3 = D - r_5 \tag{7}$$

where C_1 and S_1 mean $\cos\theta_1$ and $\sin\theta_1$, respectively.

Using Eqs. (3)-(7), F_s, F_a, r_2, θ_2 and $\theta_{2'}$ can be determined. Finally, the buckling of the middle flexure joint of the gripper can be modeled by solving Eqs. (3)-(7) numerically.

IV. FABRICATION

Smart composite microstructure (SCM)[8] fabrication process was used to replace metal-based pin joints and links with flexure joints and composite-based links. A shape memory alloy (SMA) coil actuator was installed inside the gripping structure. Due to the SCM process and SMA coil actuator, the gripper is a compact and lightweight structure.

A. Gripping Structure

The gripping structure consists of rigid links and flexure joints. Glass fiber prepreg was used for the rigid link. Copper-laminated kapton (polyimide) film was used in the flexure joint and the flexible circuit.

The SCM was fabricated using the following the process. As shown in Fig. 7(a), glass fiber prepreg was fabricated by laser micromachining. Etched copper-laminated kapton was prepared as shown in Fig. 7(b). The glass fiber prepreg and copper-laminated kapton were made into a single-layered laminate, as shown in Fig. 7(c). After curing, the SCM was fully fabricated as shown in Fig. 7(d).

Fig. 8(a) shows a 2-D pattern design for the rigid part of the gripper. The grippers were fabricated by changing the length of the middle flexure joint. Fig. 8(b) shows the fabricated

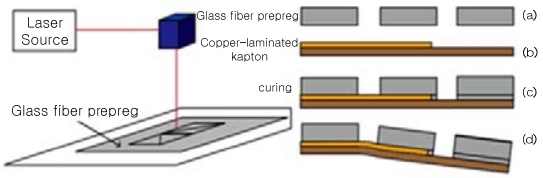

Fig. 7. Fabrication step of the SCM process. (a) Glass fiber prepreg. (b) Etched copper-laminate kapton. (c) A single-layered laminate. (d) Curing of the laminate [9].

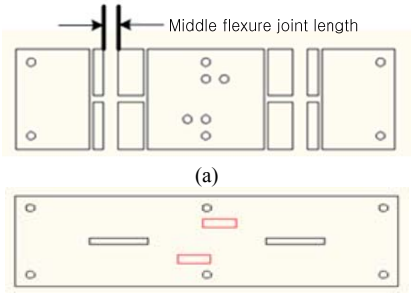

(a)

(b)

Fig. 8. (a) 2-D pattern design of the rigid link. (b) Flexible circuit pattern

copper-laminated kapton that was used as a flexible circuit. The circular holes shown in Fig. 8 were fabricated to install the SMA coil actuator through the gripping structure. The two rectangles drawn in red at the center in Fig. 8(b) represent copper in the flexible circuit.

B. Actuator

An SMA coil actuator was used to actuate the gripper. It generates force using phase transformation between martensite and austenite. When the SMA coil actuator is heated in the martensite phase, it actuates the gripper, transforming martensite into the austenite phase at 90 ℃. To use the SMA as a coil actuator, the SMA was annealed at 500℃ for 1 hr, thereby producing the desired shape of the austenite phase [13].

The spring diameter of the SMA coil actuator used in the gripper was 500,㎛ and its wire diameter was 150㎛. The spring index was 3.33. According to Eq. (8) and Eq. (9), the spring constant of the SMA coil actuator in the austenite phase is 150 N/m. We have

$$\delta = \frac{8PD^3n}{Gd^4} \tag{8}$$

$$k = \frac{Gd^4}{8D^3n} \tag{9}$$

where shear modulus G of Ni-Ti in the austenite phase is 23,000 MPa and n, the number of active coils, is 30 [14].

V. Experimental Results and Discussion

Compliant gripping is one of the most important functions of the gripping device. Other robots employ compliance and a differential mechanism for adaptive and reliable gripping or attaching [15]. For our gripper, the length of the middle flexure joint has to do with the compliance.

In this experiment, we investigated the change in compliance for various lengths of the middle flexure joint. By measuring the moment generated by the spine and the deflection angle of the middle flexure joint, the relationship between compliance and the length of the middle flexure joint was determined.

(a) (b) (c) (d)

Fig. 9. (a) Specimens of middle flexure joint, 2.5 mm and 1.5 mm.

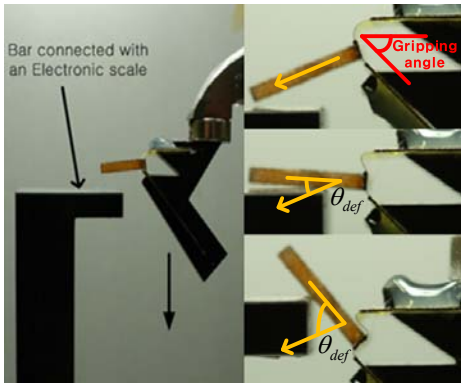

(a) (b)

Fig. 10. (a) Experimental setup. (b) Magnification of middle flexure joint. (Three arrows are parallel)

A. Experimental setup

The procedure for the experiment shown in Fig. 9 is summarized as follows:

1. Prepare middle flexure joint specimens of different lengths (0.5 mm, 1 mm, 1.5 mm, 2 mm, and 2.5 mm).
2. Prepare jigs, shown in Figs. 9(a)-(c), that keep the specimens at a specified angle. The jig angles are 45°, 90°, and 135° because the range of the gripping angle shown in Fig. 10 is 45° to 135°. Then, insert the specimens into the jigs.
3. Fig. 10(a) shows the overall experimental setup. A bar is connected to an electronic scale. Next to the bar, the specimen-inserted jig moves downward, applying force from the spine to the bar as shown in Fig. 10(b). Measure the force, and calculate the deflection angle and moment generated by the spine using ProAnalyst, a commercial video analysis tool. Next, draw the deflection angle versus moment curves.

B. Results

We assumed that:

1. The deflection angle of the spine is defined as θ_{def} , as shown in Fig. 10.
2. The deflection angle defines the compliance based on Eq. (10). That is, the larger deflection angle, the more the compliance changes:

$$\theta_{def} \propto C \tag{10}$$

where θ_{def} is the deflection angle and C is the compliance.

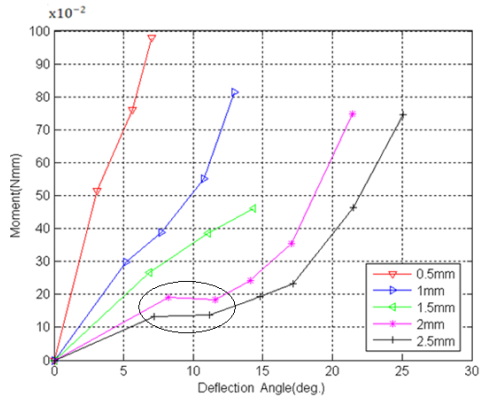

(a)

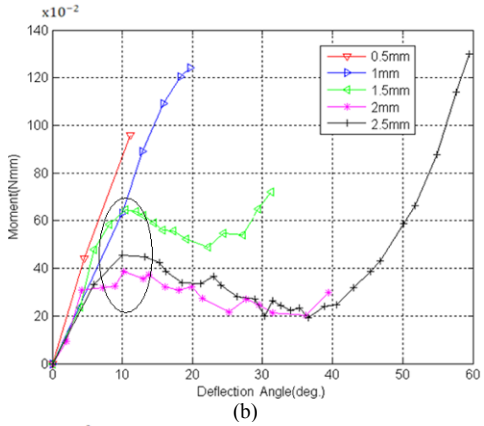

(b)

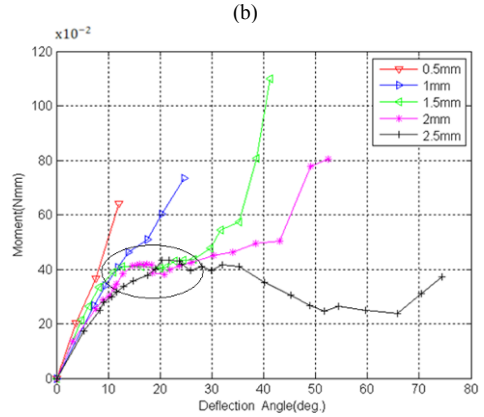

(c)

Fig. 11. Deflection angle-moment curves corresponding to gripping angle of (a) 45°, (b) 90°, and (c) 135°.

Fig. 11 shows deflection angle versus moment curves corresponding to gripping angles of 45°, 90° and 135°. As the length of the middle flexure joint increases, the maximum value of the deflection angle becomes much larger. This means that it is advantageous for the gripper to use a longer middle flexure joint. In other words, more compliant gripping can be achieved by an elongated flexure joint. The gripper can increase its compliance by gripping at a larger gripping angle. However, there is a tradeoff. There are nonlinear regions, marked as circles on the graphs, showing a sudden change in slope. This phenomenon means that excessive compliance, or too great a value of θ_{def}, may cause a failure in gripping. This

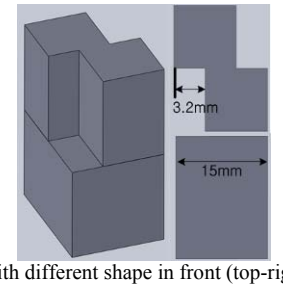

Fig. 12. Block with different shape in front (top-right) and back (top-down) side. The weight of the block is 9.8 g.

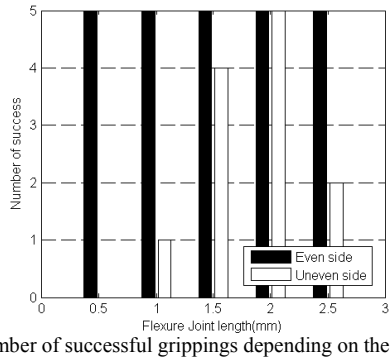

Fig. 13. Number of successful grippings depending on the length of the middle flexure joint.

phenomenon can be explained by the buckling of the middle flexure joint as shown in Fig. 15. In Fig. 15, buckling occurred at the 2 mm middle flexure joint when the gripper achieved adaptive gripping on a rough surface. Thus, we need to investigate in detail how buckling of the middle flexure joint influences compliance.

Based on our experimental data, the 1.5 mm and 2 mm middle flexure joints may be chosen as proper lengths for compliant gripping because they have rather large θ_{def} values and can overcome a sudden moment drop as the deflection angle increases.

Prototypes were built to demonstrate the experimental results and to show adaptive gripping on a block with a rough surface as shown in Fig. 12. We conducted a test with the prototypes by preparing the block weighing 9.8 g, which is 22 times heavier than the bio-inspired gripper. The block has different shapes on the front side and back side. We checked whether the gripper could lift both sides of the block. The test was repeated five times.

Fig. 13 shows results of the test. All grippers succeeded in lifting the even side of the block. However, the grippers with 0.5 mm and 1 mm middle flexure joints almost failed to lift the uneven side. This result corresponds to the experimental results that the 0.5 mm and 1 mm middle flexure joints have little compliance. On the other hand, the grippers with the 1.5 mm and 2 mm middle flexure joints lifted the uneven side of the block in more than half of the trials. The gripper with the 2 mm middle flexure joint succeeded perfectly. The gripper with the 2.5 mm middle flexure joint succeeded only twice, although it had the largest compliance. The reason may be excessive compliance. The deflection angle-moment curve for 2.5 mm in Fig. 11(c) shows that the gripper cannot overcome a sudden drop in moment caused by excessive compliance.

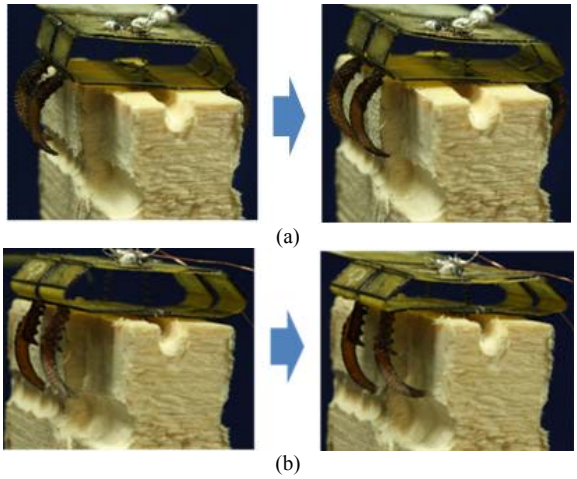

Fig. 14. Before and after gripping. (a) Gripper with 0.5 mm middle flexure joint. (b) Gripper with 2 mm middle flexure joint.

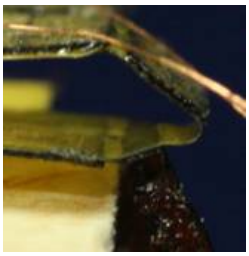

Fig. 15. Magnification of the 2 mm middle flexure joint when the gripper grips the uneven block.

Fig. 14 shows before-and-after images of gripping. Fig. 14(a) shows the gripper with a 1 mm middle flexure joint. While it cannot grip the uneven side of the block adaptively, the gripper with the 2 mm middle flexure joint grasps the uneven side with adaptive gripping as shown in Fig. 14(b). Fig. 15 is a magnification of the 2 mm middle flexure joint when the gripper grasps the uneven side. In that image, the bio-gripper is grasping the rough surface of the block adaptively with compliance by buckling of the middle flexure joint.

VI. Conclusion And Future Work

A caterpillar's proleg performs active gripping using the retractor muscle and the planta in the apical area. Inspired by the caterpillar's proleg, we presented a compact and light gripper that can be applied to small robots. An experiment provided useful information about adjusting the compliance of the gripper by changing the length of the middle flexure joint. Also, based on the test results, the prototypes showed that the bio-inspired gripper could grasp a rough surface adaptively and reliably with compliance.

Future work will include the design of a spine to enable the gripper to grasp various terrains more reliably. Specifically, the radius of the spine tip should be considered in order to grip as many asperities as possible. To achieve this, related manufacturing technologies need to be developed.

Acknowledgment

This work was financially supported by the Research Settlement Fund for the new faculty of SNU, and by the Basic Science Research Program through the National Research Foundation of Korea (NRF); the program was funded by the Ministry of Education, Science, and Technology of the Korean government (grant no. 2010K001149). The authors gratefully acknowledge this assistance.

References

[1] S. Kim, M. Spenko, S. Trujillo, B. Heyneman, D. Santos, and M.R. Cutkosky, "Smooth vertical surface climbing with directional adhesion," *IEEE Transactions on robotics*, vol. 24, 2008, pp. 65–74.

[2] M.P. Murphy and M. Sitti, "Waalbot: An agile small-scale wall-climbing robot utilizing dry elastomer adhesives," *IEEE/ASME Transactions On Mechatronics*, vol. 12, 2007, pp. 330–338.

[3] R.T. Pack, J.L. Christopher Jr, and K. Kawamura, "A rubbertuator-based structure-climbing inspection robot," *1997 IEEE International Conference on Robotics and Automation, 1997. Proceedings.*, 1997.

[4] G. La Rosa, M. Messina, G. Muscato, and R. Sinatra, "A low-cost lightweight climbing robot for the inspection of vertical surfaces," *Mechatronics*, vol. 12, 2002, pp. 71–96.

[5] K. Kotay and D. Rus, "Navigating 3d steel web structures with an inchworm robot," *Proceedings of the 1996 International Conference on Intelligent Robots and Systems, Osaka*, 1996.

[6] S. Kim, A.T. Asbeck, M.R. Cutkosky, and W.R. Provancher, "SpinybotII: climbing hard walls with compliant microspines," *12th International Conference on Advanced Robotics, 2005. ICAR'05. Proceedings., 2005,* pp. 601–606.

[7] J.S. Koh and K.J. Cho, "Omegabot: Crawling robot inspired by Ascotis Selenaria," *Robotics and Automation (ICRA), 2010 IEEE International Conference on*, 2010, pp. 109–114.

[8] R.J. Wood, S. Avadhanula, R. Sahai, E. Steltz, and R.S. Fearing, "Microrobot design using fiber reinforced composites," *Journal of Mechanical Design,* vol. 130, 2008, p. 052304.

[9] R. F. Chapman, *The Insects: Structure and Function*, 4th ed., Cambridge Universit Press, 1998, p. 175.

[10] I. Hasenfuss, "The adhesive devices in larvae of Lepidoptera (Insecta, Pterygota)," *Zoomorphology*, vol. 119, 1999, pp. 143–162.

[11] Z. Dai, S.N. Gorb, and U. Schwarz, "Roughness-dependent friction force of the tarsal claw system in the beetle Pachnoda marginata (Coleoptera, Scarabaeidae)," *Journal of Experimental Biology*, vol. 205, 2002, p. 2479

[12] Howell, L. L., 2001, *Compliant Mechanisms*, Wiley, New York

[13] K.J. Cho, E. Hawkes, C. Quinn, and R.J. Wood, "Design, fabrication and analysis of a body-caudal fin propulsion system for a microrobotic fish," *IEEE International Conference on Robotics and Automation. ICRA 2008, 2008,* pp. 706-711.

[14] K. Otsuka and C. M. Wayman, *Shape Memory Materials.* Cambridge,UK: Cambridge University Press,, 1998.

[15] A.T. Asbeck, S. Kim, M.R. Cutkosky, W.R. Provancher, and M. Lanzetta, "Scaling hard vertical surfaces with compliant microspine arrays," *The International Journal of Robotics Research*, vol. 25, 2006, p. 1165.

[16] N. D. Masters and L. L. Howell, "A self-retracting fully compliant bistable micromechanism," Microelectromechanical Systems, Journal of, vol.12, no.3, p. 273–280, 2003.

[17] N. D. Masters and L. L. Howell, "A three degree-of-freedom model for self-retracting fully compliant bistable micromechanisms," Journal of Mechanical Design, vol.127, p. 739, 2005.